Azo Polymers for Reversible Optical Storage. 5. Orientation and Dipolar Interactions of Azobenzene Side Groups in Copolymers and Blends Containing Methyl Methacrylate Structural Units

D. Brown,† A. Natansohn,*,† and P. Rochon‡

Department of Chemistry, Queen's University, Kingston, Ontario K7L 3N6, Canada, and Department of Physics, Royal Military College, Kingston, Ontario K7K 5L0, Canada

Received September 26, 1994; Revised Manuscript Received June 6, 1995®

ABSTRACT: Two amorphous copolymer series and one blend series based on Disperse Red 1 and methyl methacrylate are compared using absorption spectra and optically induced birefringence on spin-coated films. Observed blue shifts in the absorption spectra with increasing azo concentration suggest that, locally, azo dipoles are paired antiparallel both intramolecularly and intermolecularly. Induced birefringence studies indicate that the intramolecular dipolar interaction affects the orientability of the azo dipoles. The intermolecular dipolar interaction does not appear to have a large effect on orientability. The dependence of induced birefringence on azo content in the sample is different in the blend series (linear) and in the two copolymer series (nonlinear). A triad sequence distribution model is used to explain this difference. Observed writing efficiencies as a function of composition are also analyzed using a sequence distribution model. Dynamics of the inducing and birefringence relaxation processes are compared using biexponential fitting equations.

Introduction

Amorphous polymers containing substituted azobenzene groups in the side chain have been demonstrated to be good candidates for optical data storage and other electrooptic applications in part due to a mechanism that allows anisotropy to be optically induced in these materials at room temperature.[1] A review and references therein give details and examples of this mechanism and reports on possible applications.[2] The induced anisotropy manifests itself in birefringence and dichroism of long-term stability but can be eliminated by either optical or thermal means. The mechanism by which anisotropy is induced involves selective photoexcitation followed by a spatial reorientation of the azoaromatic side chain dipoles via trans–cis–trans isomerizations. By selectively exciting only dipoles possessing a sufficient dipolar component or probability of absorption in a single direction, a preferred stable dipolar orientation is created perpendicular to this direction.[1]

It is important to determine the relationship between the maximum level of anisotropy that can be induced and the concentration of the side chain chromophores in the polymeric material. As a first approximation, an independent response model where the probability of each dipole being oriented is independent on the proximity of other dipoles may be considered. This should lead to a linear relationship between the chromophore number density and the attainable anisotropy.

In the case of external electric dc field poling where the orientation of dipoles is done at temperatures above T_g, the typical theoretical description of the process is one of independent dipole response.[3] However, numerous studies in the literature indicate that the resultant orientational order is not linearly dependent on chromophore content, especially at high chromophore concentrations. Amano and co-workers[4] studying amorphous copolymers of poly[4-(3-oxopropyl)oxy)-4′-nitrostilbenyl methacrylate-*co*-methyl methacrylate] (P[MO3ONS-*co*-MMA]) found the second-order nonlinear optical (NLO) susceptibility ($\chi^{(2)}$) showed very little further increase for MO3ONS concentrations above 25 mol %. Carr et al.,[5] studying the same copolymer materials via thermally stimulated current measurements on poled thin films, found that total polarization was not linear with the chromophore number density but instead approached a plateau value at around 30 mol %. Both authors suggest that some form of dipolar interaction restricts the dipole orientation in the external electric field. This interaction increases to a concentration of about 30 mol % (65% volume fraction), above which there is little further change. Wang[6,7] and Guan[7] used an anisotropic intermolecular potential derived from a dipole–dipole orientational correlation to explain the nonlinear results of their study on a guest/host system of 2-methyl-4-nitroaniline in poly(methyl methacrylate) (PMMA). This anisotropic intermolecular interaction introduces additional functionality of the concentration into the $\chi^{(2)}$ relationship, which they relate to the correlation of electric dipoles in solution. Studies on guest/host systems of 4-(dimethylamino)-3-acetamidonitrobenzene (DAN) in PMMA carried out by Goodson and co-workers[8] indicated that the relaxation behavior of the NLO susceptibility is a function of dopant concentration. They found that the stability of the NLO susceptibility increased with increasing chromophore concentration. This behavior was not expected since as dopant concentration increases, the glass transition temperature decreases and should decrease the orientational stability of the chromophores. The enhanced stability was attributed to orientational pair correlation. In contrast to the above results, Nahata et al.,[9] studying a series of poly[4′-(((2-(methacryloyloxy)ethyl)ethyl)-amino)-4-nitroazobenzene-*co*-methyl methacrylate] (P[DR1M-*co*-MMA]) by external electric field poling and utilizing refractive index measurements, calculated NLO coefficients and found a linear relationship with the number density deviating only near the homopolymer level. Martinez et al.[10] suggest a dipole–dipole

† Queen's University.
‡ Royal Military College.
® Abstract published in *Advance ACS Abstracts,* August 1, 1995.

0024-9297/95/2228-6116$09.00/0

interaction as the cause of the deviation of SHG measurements from a thermodynamic model in electric field poling studies of an azo dye substituted acrylic polymer. With the exception of the Nahata study, it is clear that some form of dipolar interaction that increases with increased dipole concentration is affecting the orientability of chromophores.

From determination of isomerization rates from cis to trans in a series of liquid crystalline poly[6-(4-((4-cyanophenyl)azo)phenoxy)hexyl acrylate-*co*-6-(4-((4-cyanophenoxy)carbonyl)phenoxy)hexyl acrylate] copolymers in thin-film form, Wiesner[11] and co-workers observed an increase in the rate as the chromophore content increased. The greatest change in rate occurred for concentrations less than 30 mol % of the azo mer. In our lab[12] the cis–trans thermal isomerization rates were measured on copolymers P[DR1M-*co*-MMA] and poly[4'-(((2-(acryloyloxy)ethyl)ethyl)amino)-4-nitroazobenzene-*co*-methyl methacrylate] (P[DR1A-*co*-MMA]) as well as on a series of blends of PDR1A with PMMA, all in thin-film form. The results indicated a higher relaxation rate for increased chromophore content. Interestingly, the study of the isomerization for the blend series showed that rates were independent on the concentration of chromophore. Scheuermann et al.[13] using dielectric relaxation spectroscopy to study side chain liquid crystalline copolymers concluded that attaching polar mesogenic groups on the side chain enhanced the dipolar interaction. This interaction manifested itself as an apparent increase in the dipole moments as the dipole concentration increased. It seems reasonable therefore to expect that some form of dipolar interaction which increases with the concentration of chromophore should be expected in optically induced anisotropy studies as well.

There are no studies in the literature carried out on series of dipolar side chain homopolymers blended with nonphotoactive polymers that would indicate if dipolar interactions are present. It should be possible to discern between intramolecular interactions and intermolecular interactions by comparing a copolymer series and blend series. This paper presents the results of absorbance and induced birefringence measurements on two series of copolymers and one series of blends. They are interpreted as evidence for side chain intramolecular dipolar interaction.

Experimental Section

The synthesis and characterization of the two series of copolymers P[DR1A-*co*-MMA] and P[DR1M-*co*-MMA] and the blend series PDR1A-*blend*-PMMA have been described in previous publications.[14-16] The general formula of all samples is presented in Chart 1. Compositions and T_g values for the samples used can be found in Table 1. All blends are compatible at the molecular level.[15] Films of these series were prepared by spin casting from tetrahydrofuran onto clean glass microscope slides which were subsequently heated to drive off THF. Optical anisotropy was induced using a linearly polarized 488 nm, 20 mW argon beam and measured using a diode laser beam at 751 nm. Film thicknesses ranging from 100 to 1000 nm were determined by measuring the displacement of interference fringes produced by light reflected from the film surface with respect to those produced by light which is reflected from the glass substrate. The resultant thicknesses were used to calculate the birefringence from the measured phase shift. Absorption coefficients at 488 nm were determined using a circularly polarized argon beam on a previously unexposed area of the films. All measurements were carried out at room temperature. Densities were determined for cast films removed from their glass substrate in calcium nitrate solution at 22 °C by adjusting the density until a stable suspension was achieved and then measuring the density of the solution with a pycnometer. UV absorption spectra were measured on a Hewlett-Packard 8452A diode array spectrophotometer using the prepared film samples. Compositions of the samples were determined by ^{1}H NMR solution spectra. Using composition and conversion data, triad sequence distributions were calculated as reported previously.[16]

Chart 1

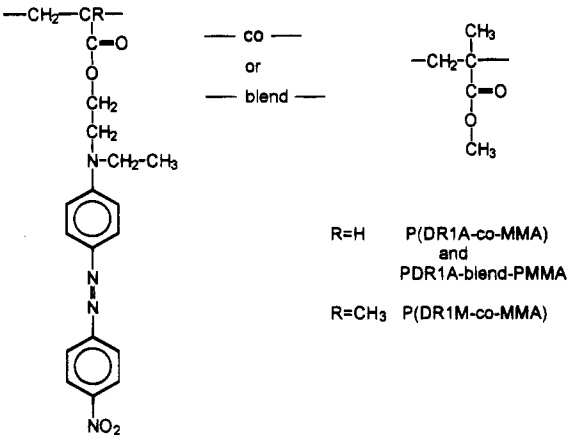

Table 1. Glass Transition Temperatures of Copolymer and Blend Samples

sample	azo mol frac	wt frac	T_g (°C)
P(DR1A-*co*-MMA)	1	1	91
	0.81	0.94	102
	0.69	0.89	95
	0.57	0.83	94
	0.44	0.74	91
	0.35	0.66	89
	0.23	0.51	91
	0.12	0.34	92
	0.08	0.27	
	0.04	0.13	
	0.02	0.07	
	0.01	0.04	
	0.005	0.02	
P(DR1M)-*co*-MMA)	1	1	129
	0.82	0.94	122
	0.65	0.88	119
	0.46	0.76	120
	0.36	0.68	120
	0.28	0.60	120
	0.17	0.44	110
	0.12	0.35	112
	0.06	0.19	114
PDR1A-*blend*-PMMA	0.88	0.96	92
	0.75	0.92	90
	0.62	0.86	91
	0.50	0.79	91
	0.38	0.69	92
	0.25	0.55	91
	0.12	0.34	91
	0.08	0.24	
	0.04	0.13	
	0.02	0.07	
	0.01	0.04	
	0.005	0.02	

Results and Discussion

Figure 1 gives a typical write–erase profile of optically induced and subsequently eliminated birefringence for the PDR1A homopolymer. We refer to this as writing and erasing on the polymer film. At point A the plane polarized write beam is engaged and birefringence is rapidly induced up to the maximum or saturation level where the rate of change of anisotropy becomes very small (point B). This level is maintained

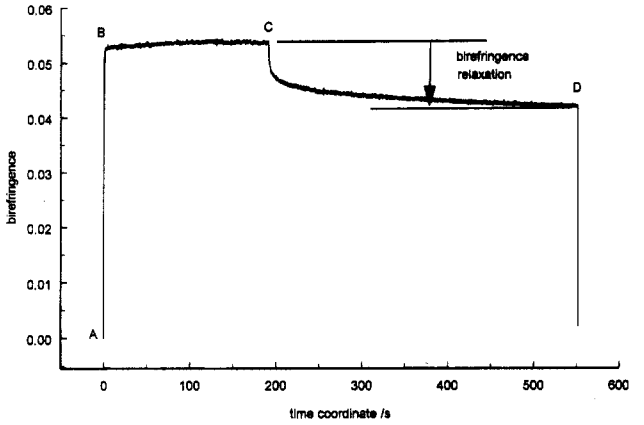

Figure 1. Write–erase profile of optically induced and erased birefringence: (A) write beam on; (B) saturation attained; (C) write beam off, (D) erase beam on.

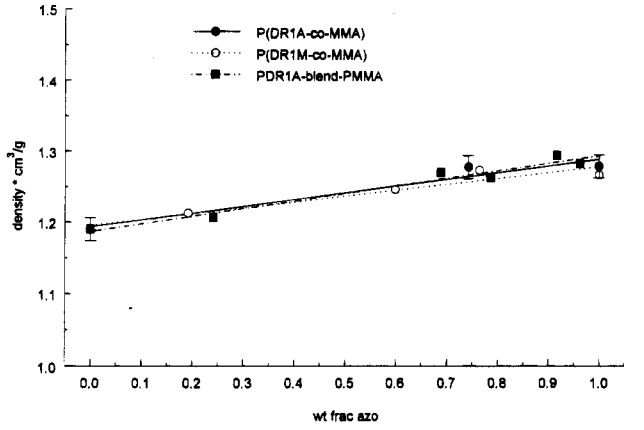

Figure 2. Densities of the three polymer series as a function of azo weight fraction. Curves are drawn to guide the eye. Error bars are given for the P(DR1A-*co*-MMA) series.

until the write beam is terminated at point C and the birefringence falls off exponentially to a relaxed level where the rate of change of anisotropy is again very small (point D). At point D the circularly polarized erase beam is turned on and eliminates the birefringence of the written area.

The results of density measurements can be found in Figure 2. The increase in density as the azo concentration increases appears to be linear and similar for each series within experimental limitations. Nahata et al.[9] obtained similar results for the densities of a P(DR1M-*co*-MMA) series. From the material densities and the weight fraction of azo mers, number densities of chromophores per unit volume were determined.

The dipole birefringence or birefringence per dipole is defined as the net birefringence observed at C in Figure 1 divided by the number density of azo dipoles in the polymer sample. This then represents the average orientation contribution that each dipole in the sample makes to the macroscopically observed birefringence.

(A) Absorption Spectra. The absorption spectra for selected samples from the DR1A-containing series are shown in Figure 3. Both copolymer series show a systematic shift of the absorption maxima to shorter wavelength as the azo concentration increases. The shift is accompanied by a slight broadening of the band. Examination of the blend spectra reveal the same shift to shorter wavelengths but it is less pronounced, approximately 10 nm as compared to 22 nm in the copolymers. This can be clearly seen in Figure 3c.

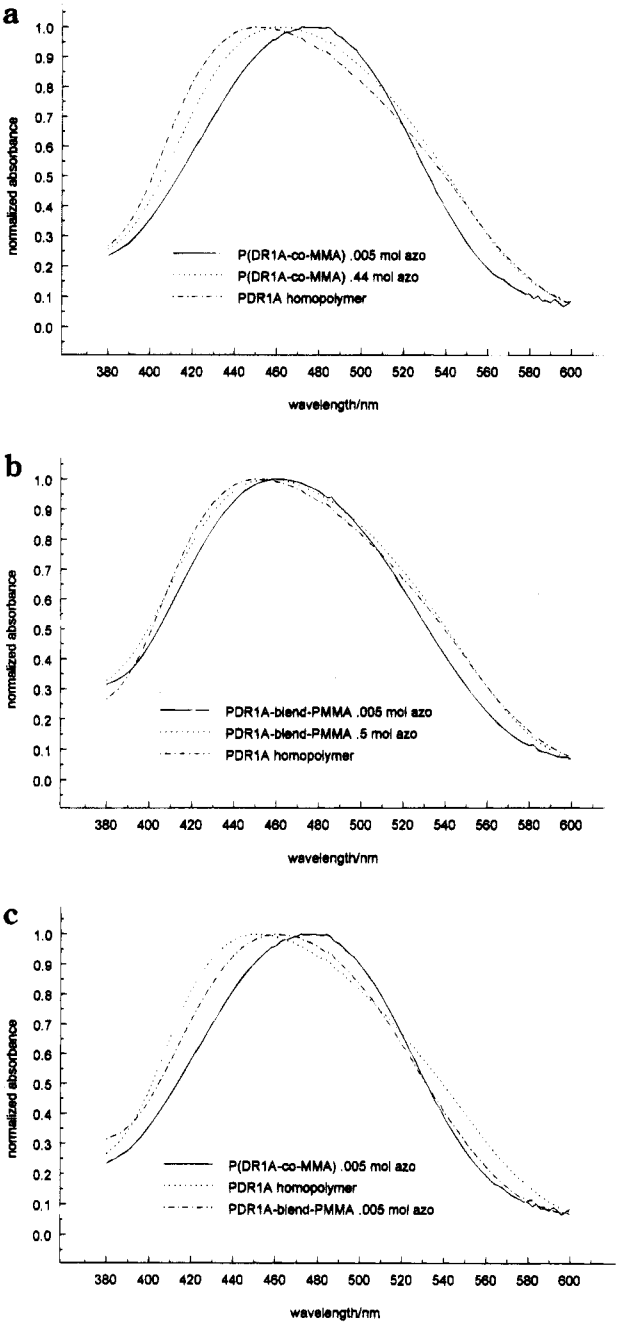

Figure 3. (a) Comparison of absorbances for two copolymer samples and the homopolymer PDR1A. (b) Comparison of absorbances for two blend samples and the homopolymer PDR1A. (c) Comparison of absorbances for a copolymer sample a blend sample and the homopolymer PDR1A.

There are examples in the literature of shifts in absorption maxima and band broadening for copolymers containing chromophores in the side chain and systems of dye molecules dissolved in solid polymer matrices. The shifts are to longer wavelength and are usually the result of application of an external electric poling field. Wedel et al.[17] poled samples of a copolymer of methacryloyl anhydride with 4′-(((2-(methacryloxy)hexyl)-ethyl)amino)-4-nitroazobenzene as well as the same structural units in a copolymer with methyl methacrylate and observed shifts in the absorption maxima of up to 13 nm between unpoled and poled samples. Tsutsumi and coworkers[18] reported spectral shifts to longer wavelengths in poled samples of 4-(dimethylamino)-4′-nitrostilbene (DANS) dissolved in blends of vinylidene fluoride and trifluoroethylene copolymer

(P[VDF–TrFE]) with PMMA. The spectral shifts have been assigned to development of a local internal electric field caused by parallel dipole alignment. This is an extension of the theory of electrochromic effects in liquid solutions developed by Liptay and co-workers.[19] The theory describes the energy difference between a ground and an excited state in the presence of an electric field as being reduced proportional to the product of strength of the field, the difference in dipole moments between the two states, and the cosine of the angle between the field and the dipole.

In the case where dipoles are aligned parallel, the resulting local electric field will be in the same direction as the dipoles and hence the cosine of the angle between dipoles will be positive, reducing the absorption energy. If this same theory is to be used to explain spectral shifts to higher absorption energies, the value of the cosine must be negative. This would imply that dipoles are antiparallel with each other. Eckhardt et al.[20] observed a blue shift with increasing concentration of merocyanine dissolved in a polymer matrix. This was attributed to formation of aggregates in which the dipoles are associated in an antiparallel arrangement.

UV absorption studies on solutions of polymers with dipolar side groups have also shown a blue shift with increasing dipole concentration. Goldburt and coworkers[21] observed a blue shift in copolymers containing a merocyanine side group. They attributed this to antiparallel dipolar aggregates formed by polymer chains looping around such that the side chains can interdigitate. Altomare et al.[22] studied copolymers of 4-(acryloxy)azobenzene with (−)-menthyl acrylate and also observed a shift to shorter wavelengths in the solution UV absorption spectra as the concentration of azobenzene side chains increased. These studies suggest that an antiparallel association of neighboring dipoles is a viable explanation for the blue shift observed in the absorption data reported here.

In terms of sequence distribution, at low azo concentrations the polymer contains primarily isolated dipoles or MDM (methyl methacrylate, DR1, methyl methacrylate) triads. These dipoles will experience no local field since they are isolated from other dipoles. As the azo concentration increases there is increasing occurrence of azo-centered triads with one neighboring dipole (MDD) and triads with two neighboring dipoles (DDD). The dipole in the MDD triad will experience an electric field from its neighbor. The central dipole in the DDD triad will experience a resultant electric field due to two adjacent azo groups. If adjacent dipoles are associated in an antiparallel arrangement, as concentration increases the local field felt by the azo groups will increase and the average field would be weighted according to the sequence distribution of the three types of triad at that particular concentration. The blend series contains only homopolymer chains; hence each dipole has two neighbors (excluding end groups) and no sequence distribution effect should be observed. This argument implies that dipolar association occurs mainly intramolecularly between dipoles on the same chain. However, there must be some intermolecular association as well since there is a blue shift seen, albeit smaller, in the blend series as well. It seems reasonable to conclude that the intramolecular effect is responsible for the difference in absorption maxima observed between low azo concentration blends and copolymers of comparable composition. The remainder of the blue shift between these low azo concentration blends and the pure homopolymer must result from an intermolecular concentration effect which should be expected due to the closer proximity of dipoles as concentration is increased.

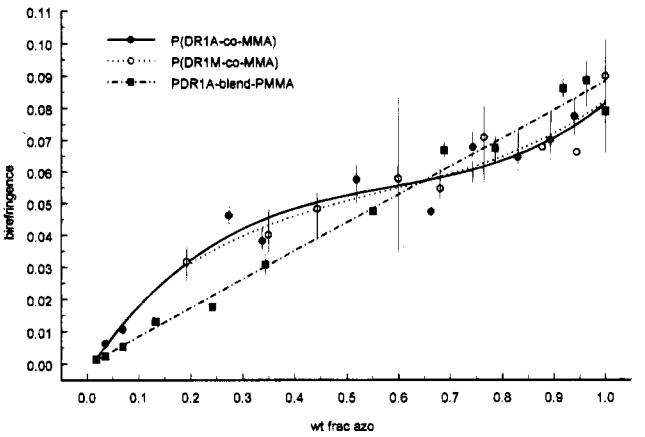

Figure 4. Maximum induced birefringence values for the three polymer series plotted as a function of azo weight fraction. Curves are drawn to guide the eye. High–low values are indicated by the vertical lines.

It would be expected that antiparallel association of adjacent dipoles in a copolymer would be more favorable for racemic diads since the dipoles could point in opposite directions from the chain with less stress. Previously published data on the tacticity of P(DR1M-*co*-MMA) indicate that as the azo concentration increases, the probability of occurrence of racemic diads decreases slightly.[16] It must be expected that the tacticity will play some role in the intramolecular association, but lack of tacticity information prevents any conclusions from being drawn. It would be necessary to prepare a similar polymer with strict tacticity control during synthesis to explore tacticity effects.

(B) Birefringence. The maximum achieved birefringence for each series is plotted as a function of azo weight fraction in Figure 4. The plot is a function of weight fraction because the laser beam used to detect the birefringence illuminates a constant area and therefore measured birefringence values are for a constant volume of material. Variations in the density of the material with composition will be reflected in the data. The density is linear with weight fraction as demonstrated earlier and hence any deviations from linearity are not density related. The blend birefringence increases linearly with the azo weight fraction. The two copolymers achieve higher birefringences than the blends at low and mid-range concentrations, with the homopolymers having the highest birefringence of all. The birefringence per dipole data are plotted as a function of mole fraction in Figure 5. As this is not a bulk property anymore but reflects molecular-level phenomena, it would not be appropriate to use weight fractions here. This figure shows the dipole birefringence for the blend series to be constant at essentially the level of the homopolymer while the copolymers have a higher dipole birefringence at low azo concentration values which gradually decreases with increasing concentration. At concentrations of 0.45 mol and higher the birefringence per dipole becomes essentially constant. The fact that the blend dipole birefringence is constant across the series indicates that the intermolecular interaction attributed to the blue shift in the blend absorbance data is probably not a large factor in orientability. The variation in dipole birefringence observed for the copolymer series must therefore be a

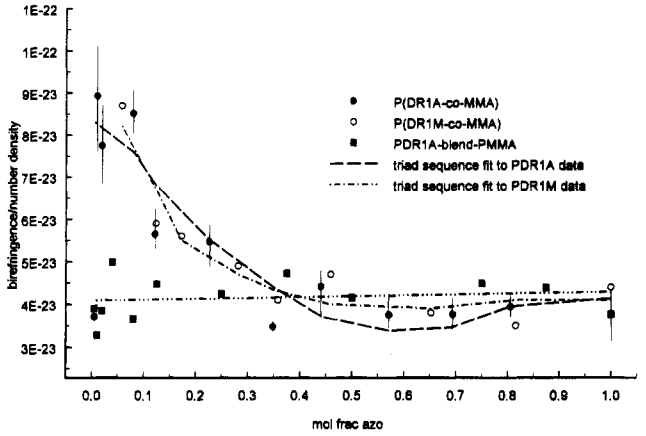

Figure 5. Birefringence values divided by number density showing contribution to observed birefringence per azo group. Triad sequence distribution fit procedures are described in the text. Curves are drawn to guide the eye. Sample error bars are given for one of the series.

result of intramolecular association. As discussed in the previous section, absorbance data predict intramolecular antiparallel association with each type of central azo experiencing a different local electric field. The isolated azo group should "see" no field and the azo groups with one and two adjacent dipoles should experience resultant fields depending on the number and orientation of neighboring dipoles. The blend series contains only DDD triads at all azo concentrations. Thus an essentially constant dipole birefringence is exhibited across the blend series which correponds to the value observed for the homopolymer. The variation of dipole birefringence across the copolymer series may be modeled by using a weighted proportion of the three different triads. A least squares fit of the following equation was attempted for the two copolymer series data sets.

$$\mathrm{DB} = Xf_{\mathrm{MDM}} + Yf_{\mathrm{MDD}} + Zf_{\mathrm{DDD}} \qquad (1)$$

Here DB is the dipole birefringence, the f's are the normalized triad fractions, and X, Y, and Z are fit parameters representing the relative orientabilities of the central azo group in each triad. The resulting fitted curves for the two copolymer series having different sequence distributions can be seen in Figure 5 and the fit parameters are as follows:

series	fit parameters ($\times 10^{-23}$) $X_{(\mathrm{MDM})}$	$Y_{(\mathrm{MDD})}$	$Z_{(\mathrm{DDD})}$	correl coeff
P(DR1A-*co*-MMA)	8.3	0.54	4.9	0.95
P(DR1M-*co*-MMA)	10.1	1.9	4.5	0.95

The correlation coefficient gives an indication of the reliability of the fit. The 0.005 mol azo P(DR1A-*co*-MMA) sample was omitted from the fitting. The results indicate that the azo group with only one neighboring dipole gives the smallest contribution to the birefringence, and the isolated dipole gives the highest contribution. This suggests that the order of relative optical orientability is MDM > DDD > MDD. In other words, a dipole with one neighbor is more likely to remain in its original position than a dipole having two neighbors which is in turn more likely to remain in its original position than an isolated dipole. A simple model would predict that an azo group paired antiparallel with two dipoles should be held more strongly than if it were only paired with another one, producing a relative reorientability order of MDM > MDD > DDD. All attempts to fit the data according to such an orientability order were unsuccessful.

Table 2. Relax Curve Biexponential Fitting Results

sample	azo mol frac	C_n	D_n	E_n	k_c	k_d
P(DR1A-*co*-MMA)	1.00	0.09	0.09	0.81	2.04	0.09
	0.81	0.14	0.10	0.76	1.98	0.11
	0.69	0.07	0.09	0.84	1.63	0.08
	0.57	0.11	0.12	0.77	1.51	0.09
	0.44	0.12	0.11	0.77	2.05	0.09
	0.35	0.13	0.12	0.75	1.51	0.09
	0.23	0.15	0.14	0.70	1.69	0.10
	0.12	0.12	0.11	0.77	1.60	0.08
	0.08	0.11	0.11	0.77	1.86	0.08
	0.02	0.08	0.10	0.82	1.61	0.07
	0.01	0.15	0.20	0.65	1.39	0.07
	0.005	0.24	0.24	0.53	1.98	0.09
P(DR1M-*co*-MMA)	1.00	0.09	0.09	0.82	3.07	0.07
	0.82	0.14	0.11	0.75	2.28	0.09
	0.65	0.10	0.08	0.82	2.01	0.08
	0.46	0.10	0.11	0.79	1.73	0.08
	0.46	0.11	0.11	0.78	1.87	0.08
	0.36	0.06	0.10	0.84	1.56	0.06
	0.28	0.09	0.10	0.81	3.19	0.07
	0.17	0.06	0.11	0.83	1.33	0.07
	0.12	0.08	0.10	0.82	2.06	0.07
	0.06	0.07	0.07	0.86	2.27	0.06
PDR1A-*blend*-PMMA	1.00	0.09	0.09	0.81	2.04	0.09
	0.88	0.10	0.07	0.83	2.62	0.09
	0.75	0.11	0.08	0.81	1.96	0.10
	0.50	0.10	0.07	0.83	2.40	0.09
	0.38	0.14	0.11	0.75	2.19	0.09
	0.38	0.12	0.10	0.78	1.97	0.10
	0.25	0.12	0.09	0.78	1.98	0.09
	0.13	0.13	0.10	0.76	2.02	0.07
	0.08	0.10	0.10	0.80	1.81	0.09
	0.04	0.14	0.12	0.75	1.99	0.09
	0.02	0.10	0.12	0.77	1.80	0.09
	0.02	0.16	0.14	0.71	2.23	0.09
	0.01	0.13	0.14	0.74	1.98	0.09
	0.005	0.12	0.15	0.74	1.99	0.09

(C) Relaxation Behavior. Upon termination of the write beam, birefringence levels fall off from the saturation level to a relaxed level. This is probably due to thermally activated dipole reorientation which will tend toward randomization of the anisotropy. A slight contribution to relaxation may arise from cis isomers with significant dipolar components oriented perpendicular to the polarization plane, isomerizing back to the trans form and reorienting.

The relaxation curve can be fit very well with the following biexponential function where Δn is the birefringence.

$$\Delta n = C \exp(-k_c t) + D \exp(-k_d t) + E \qquad (2)$$

Although detailed relaxation mechanisms are unknown, parameters extracted from fitting the relaxation curves with this equation can be used to compare the copolymers and blends studied here. The equation describes two exponential relaxation modes, one "fast" and the other "slow", represented by the terms $C \exp(-k_c t)$ and $D \exp(-k_d t)$, respectively. The "fast" decay, having contribution C and time constant k_c, can be attributed to thermal cis–trans isomerization and dipole reorientation. The "slow" decay, with contribution D and time constant k_d, is attributed to slower dipole reorientation, probably involving motions of the main chain of the polymer. The E parameter represents the birefringence remaining after infinite time.[23] The normalized E ($E_n = E/\{C + D + E\}$) is the fraction of the maximum birefringence conserved. Results of fitting the biexpo-

nential equation can be found in Table 2. For both the copolymer series and the blend series, E_n appears essentially constant at approximately 0.8 with the exception of copolymer samples of concentration 0.01 mol azo and below, which have values of 0.65 and 0.53, respectively. Normalized values of C and D are constant at approximately 0.1 for each with the exception of the samples of 0.01 mol azo and below, which have values of about 0.2. The relaxation time constants k_c and k_d extracted from the relaxation curve fitting also appear to be constant with azo concentration, having values of approximately 2 and 0.1 s^{-1}, respectively, including the low-concentration copolymer samples. These constant levels seen for both copolymers and blends indicate that the birefringence relaxation is not affected by the sequence distribution of the polymer. It is unclear why copolymer samples of 0.01 mol fraction azo and below appear to decay more than the others. This will be further discussed with write curve fitting results.

It is of relevance here to comment on the results of Walsh and co-workers.[24] They studied the long-term (up to 6×10^4 s) relaxation of poled order in samples of P[DR1M-*co*-MMA] and a similar copolymer using 4-amino-4′-nitrotolane (NAT) in place of DR1. The relaxation behavior was found to follow the same trends as similar guest/host systems for temperatures above $T_g - 50$. Below $T_g - 50$, however, the relaxation was slower than for the guest/host system. The T_g's of our copolymer samples range from 90 to 120 °C; hence at room temperature they are below this break point. Since the break point is related to the T_g, thus the main chain motion in the polymer, it follows that the relaxation behavior should be largely independent of side chain dipole concentration.

(D) Efficiency. The writing times for each sample can be used to calculate an efficiency defined as anisotropy achieved per energy absorbed. This is done by taking the achieved anisotropy ($\Delta n_m d$, where Δn_m is the maximum achieved birefringence and d is the sample thickness) once the saturation plateau has been reached and dividing by the absorbed laser power (P) (obtained from the laser power, the sample optical density, and the illuminated area) times the time required to reach 95% of the saturation level. 95% of the saturation level was chosen because it is impossible to determine the exact time when 100% saturation is achieved.

$$\Phi = \frac{\Delta n_m d}{Pt} \tag{3}$$

Since writing rates are a function of film thickness, only samples of similar optical density can be compared.[25] For this to be true, the value of the absorption coefficient times the sample thicknesses must agree between samples. Hence lower concentrations of the azo absorbing species require thicker films for the efficiency comparison. The efficiency calculations are given in Figure 6 as a function of azo mole fraction. The broad scatter in this data results from the difficulty of spin coating films of closely controlled thickness. Hence the optical densities of the samples vary. General trends exhibited by the efficiency calculations should, however, still be valid.

Results indicate that all blend samples exhibit similar efficiencies that correspond to that of the PDR1A homopolymer. The P(DR1A-*co*-MMA) series shows a variation of efficiency value with azo concentration. Samples of 0.02 mol azo and below have very low values, below that of the homopolymer and the blends. The rest of the P(DR1A-*co*-MMA) series have values higher than the homopolymer, which decrease as azo concentration increases. The efficiency values for the P(DR1M-*co*-MMA) series are broadly scattered and no trend can be identified. The anomalous values of the very low concentration P(DR1A-*co*-MMA) samples originate from write curves that exhibit different dynamics than the rest of the samples. This will be discussed in the next section.

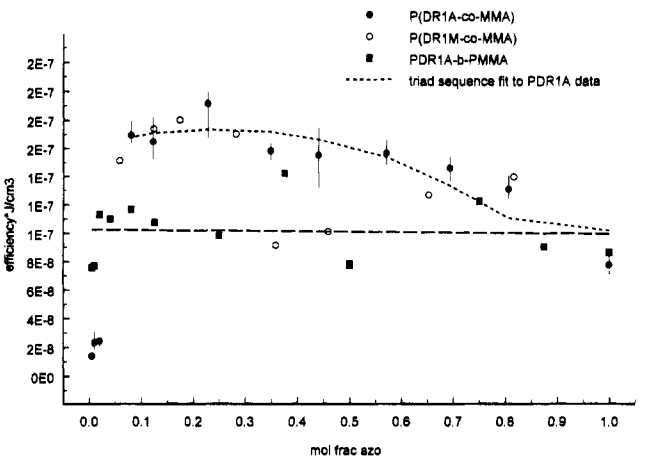

Figure 6. Efficiency of the optical reorientation process defined as anisotropy achieved per energy absorbed. Triad sequence distribution fit is described in the text. Curves are drawn to guide the eye. Sample error bars are given for one of the series.

A least squares fit of the efficiency data of the P(DR1A-*co*-MMA) series with the triad sequence distribution data (eq 1) can be found in Figure 6. The fit was calculated omitting the three lowest concentration points. In this case the fit parameters X, Y, and Z represent the relative efficiencies of the central azo group in each triad. The broad scatter of the efficiency data for the P(DR1M-*co*-MMA) prevented modeling of that data set. The results for the P(DR1A-*co*-MMA) series are as follows:

	efficiency fit parameters ($\times 10^{-7}$)			correl coeff
	$X_{(MDM)}$	$Y_{(MDD)}$	$Z_{(DDD)}$	
P(DR1A-*co*-MMA)	1.6	2.0	0.82	0.88

These results indicate that azo groups with one neighboring azo are the most efficiently oriented followed by the isolated dipoles, azo groups having two neighboring dipoles being the least efficiently oriented. Overall, the efficiency reflects two competing phenomena, the orientation of azo groups and relaxation of groups that have been oriented and which are still under illumination. The fitting results imply that the ratio of the orientation rate to the relaxation rate is greatest for the MDD triad and least for the DDD triad. Note that this order, MDD > MDM > DDD, differs from the dipole birefringence contribution order. The MDD triad has the smallest contribution to the dipole birefringence but the largest contribution to the efficiency. In combination, these two sequence fitting results indicate a higher orientational stability exhibited by the MDD triads. They are more difficult to orient, and hence less of them will, but once they are oriented, they are less likely to relax back to the original position. This reduces the rate of relaxation during the writing process, increasing the orientation rate to relaxation rate ratio and hence the efficiency.

Table 3. Write Curve Biexponential Fitting Results

sample	azo mol frac	A_n	B_n	k_a	k_b
P(DR1A-*co*-MMA)	1.00	0.80	0.20	4.05	0.50
	0.81	0.93	0.08	4.79	0.18
	0.69	0.88	0.12	4.32	0.29
	0.57	0.89	0.11	4.50	0.56
	0.44	0.95	0.05	4.98	0.13
	0.35	0.90	0.10	4.51	0.68
	0.23	0.92	0.08	4.56	0.26
	0.12	0.94	0.07	4.14	0.26
	0.08	0.92	0.08	3.90	0.27
	0.02	0.63	0.37	3.71	0.63
	0.01	0.50	0.50	4.91	1.18
	0.005	0.74	0.26	4.08	0.25
P(DR1M-*co*-MMA)	1.00	0.91	0.09	4.25	0.58
	0.82	0.96	0.04	4.82	0.16
	0.65	0.86	0.14	3.91	0.59
	0.46	0.88	0.12	3.85	0.48
	0.46	0.85	0.15	4.72	1.11
	0.36	0.77	0.24	3.37	0.64
	0.28	0.81	0.19	4.15	0.20
	0.17	0.96	0.04	4.36	0.67
	0.12	0.96	0.04	4.02	0.63
	0.06	0.86	0.14	3.55	1.03
PDR1A-*blend*-PMMA	0.88	0.75	0.25	3.90	0.19
	0.75	0.77	0.23	3.86	0.39
	0.50	0.73	0.27	3.29	0.42
	0.38	0.97	0.03	4.75	0.13
	0.38	0.84	0.16	4.13	0.66
	0.25	0.77	0.23	3.80	0.36
	0.13	0.83	0.17	4.44	0.17
	0.08	0.82	0.18	3.94	0.39
	0.04	0.78	0.22	5.19	0.77
	0.02	0.82	0.18	4.16	0.23
	0.02	0.89	0.11	4.85	0.42
	0.01	0.80	0.20	4.12	0.24
	0.005	0.79	0.21	4.11	0.25

(E) Write Curve Fitting. The write curves can be fit with the following biexponential equation:

$$\Delta n = A(1 - \exp(-k_a t)) + B(1 - \exp(-k_b t)) \quad (4)$$

where Δn is the birefringence, k_a and k_b are time constants, and A and B are the birefringence contributions of each of the exponential response modes. Parameters extracted from fitting this equation can be used to compare the materials studied.[23] In a similar manner to the birefringence decay, the writing behavior exhibits a "fast" response and a "slow" response represented by the terms $A(1 - \exp(-k_a t))$ and $B(1 - \exp(-k_b t))$, respectively. The "fast" response mode can be attributed to dipole reorientation through trans–cis–trans isomerizations and the "slow" component to accommodating motions of the polymer main chain. This model should not be misunderstood to imply that there are two distinctive writing mechanisms in play with well-defined time constants; rather the biexponential is an approximation for a multiplicity of writing rates.

Fitting results presented in Table 3 show that the time constants k_a and k_b remain constant with azo concentration for all of the three series studied, at levels of approximately 4.5 and 0.5 s^{-1}, respectively. It is important that the optical densities of the films compared be similar as was the case for the efficiency comparison since greater values of optical density yield smaller values for the time constants. The contributions A and B of each of the exponential terms of the fitting equation can be normalized to a fraction contribution by dividing each by their sum. Results give values of A_n and B_n of approximately 0.9 and 0.1, respectively, for all samples except the copolymer samples of 0.02 mol azo and below. The independence of both the time constants and the birefringence contribution of the two processes on azo concentration suggests that the writing dynamics are not affected by the sequence distribution of the polymer.

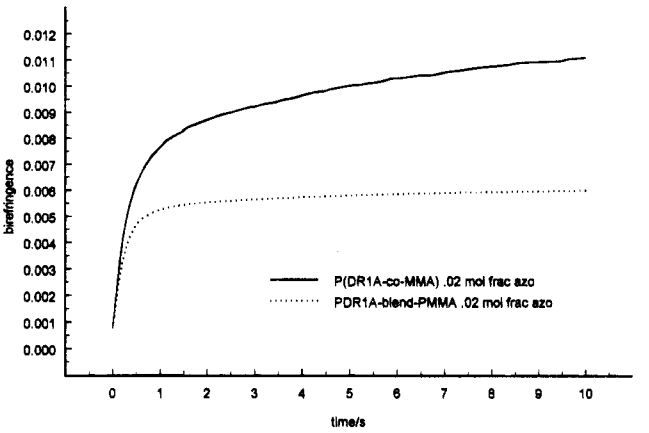

Figure 7. Comparison of the write curves of 0.02 mol azo P(DR1A-*co*-MMA) and 0.02 mol azo PDR1A-*blend*-PMMA.

The contribution values for the copolymer samples below 0.02 mol fraction azo vary from 0.5 to 0.75 for A_n. Figure 7 compares the write curves of a 0.02 mol azo blend and copolymer. It is clear that the dynamics of the writing process are quite different between these two samples, with the copolymer not achieving saturation within the time plotted. This is the reason for the low efficiency values exhibited by these samples. The copolymers in this range also showed much lower fractions of the maximum birefringence conserved. Interestingly, the blend samples in this concentration range show no deviation in either the writing or relaxation behavior. All of these results suggest that there is some significant difference of the reorientation dynamics between copolymers and blends within this very low azo concentration range. This may be due to the predominance of MDM triads (isolated azo dipoles). Blend samples would not show the same behavior since the dipoles are in DDD sequences exclusively. This is supported by the blue shift of the absorption spectra from the 0.005 mol azo copolymer to the 0.005 mol azo blend seen in Figure 3c.

Conclusions

There is some form of dipolar interaction between the azo groups on the side chains that are next to each other on the polymer backbone. Absorption maxima shifts to higher energy with increasing azo concentration indicate that the dipoles are associated in an antiparallel fashion. This interaction reduces the mobility of the side chain but enhances the orientational stability.

Since the interaction effect on orientation seems to be mainly intramolecular, the macroscopically observed net orientation properties depend mainly on the sequence distribution of the copolymer. Sequence distribution analysis of the data indicates that the isolated azo group of the MDM triad has the highest weighted contribution to the maximum achievable birefringence. The highest levels of induced birefringence are obtained for homopolymers; however, birefringence is more efficiently induced in copolymers between 0.02 and 0.08 mol azo. Copolymers below this concentration exhibit different orientation dynamics than the rest of the samples. When utilizing the homopolymers in blends, the birefringence is a linear function of the azo number

density with the efficiencies similar to that of the homopolymer.

Acknowledgment. We thank the Office of Naval Research, NSERC Canada, and the Department of National Defence Canada for funding. Dr. S. Xie is acknowledged for synthesizing the materials used in this study.

References and Notes

(1) Rochon, P.; Gosselin, J.; Natansohn, A.; Xie, S. *Appl. Phys. Lett.* **1992**, *60*, 4.
(2) Xie, S.; Natansohn, A.; Rochon, P. *Chem. Mater.* **1993**, *5*, 403.
(3) *Materials for Nonlinear Optics, Chemical Perspectives*; Marder, S. R., Sohn, J. E., Stucky, G. D., Eds.; American Chemical Society: Washington, D. C., 1991.
(4) Amano, M.; Kaino, T.; Yamamoto, F.; Takeuchi, Y. *Mol. Cryst. Liq. Cryst.* **1990**, *182A*, 81.
(5) Carr, P. L.; Davies, G. R.; Ward, I. M. *Polymer* **1993**, *34*, 5.
(6) Wang, C. H. *J. Chem. Phys.* **1993**, *98*, 3457.
(7) Guan, H. W.; Wang, C. H. *J. Chem. Phys.* **1993**, *98*, 3463.
(8) Goodson, T., III. Gong, S. S.; Wang, C. H. *Macromolecules* **1994**, *27*, 4278.
(9) Nahata, A.; Shan, J.; Yardley, J. T.; Wu, C. *J. Opt. Soc. Am. B* **1993**, *10*, 1553.
(10) Martinez, D. R.; Koch, K.; Ratsavong, F. K.; Carlisle, G. O. *J. Appl. Phys.* **1994**, *75*, 4273.
(11) Wiesner, U.; Antonietti, M.; Boeffel, C.; Spiess, H. W. *Makromol. Chem.* **1990**, *191*, 2133.
(12) Barrett, C.; Natansohn, A.; Rochon, P. *Macromolecules* **1994**, *27*, 4781.
(13) Scheuermann, H.; Tsukruk, V.; Finklemann, H. *Liq. Cryst.* **1993**, *14*, 889.
(14) Natansohn, A.; Rochon, P.; Gosselin, J.; Xie, S. *Macromolecules* **1992**, *25*, 2268.
(15) Xie, S.; Natansohn, A.; Rochon, P. *Macromolecules* **1994**, *27*, 1489.
(16) Xie, S.; Natansohn, A.; Rochon, P. *Macromolecules* **1994**, *27*, 1885.
(17) Wedel, A.; Strohriegl, P.; Danz, R. *Acta Polym.* **1993**, *44*, 302.
(18) Tsutsumi, N.; Ono, T.; Kiyotsukuri, T. *Macromolecules* **1993**, *26*, 5447.
(19) Liptay, W. In *Excited States*; Lim, E. C., Ed.; Academic Press: New York, London, 1974; Vol. I, pp 129–229.
(20) Eckhardt, H.; Bose, A.; Krongauz, V. A. *Polymer* **1987**, *28*, 1959.
(21) Goldburt, E.; Shvartsman, F.; Fishman, S.; Krongauz, V. *Macromolecules* **1984**, *17*, 1225.
(22) Altomare, A.; Carlini, F.; Ciardelli, F.; Solaro, R. *J. Polym. Sci., Polym. Chem. Ed.* **1984**, *22*, 1367.
(23) Ho, M. S.; Natansohn, A.; Rochon, P. *Macromolecules* **1995**, *28*, 6124.
(24) Walsh, C. A.; Burland, D. M.; Lee, V. Y.; Miller, R. D.; Smith, B. A.; Twieg, R. J.; Volksen, W. *Macromolecules* **1993**, *26*, 3720.
(25) Rochon, P.; Bissonnette, D.; Natansohn, A.; Xie, S. *Appl. Opt.* **1993**, *32*, 7277.

MA946356A